La mer 37 : 145-152, 2000
Société franco-japonaise d'océanographie, Tokyo

Observation of tidal and residual circulations in Osaka Bay by HF radar

Satoru TAKAHASHI*, Ichiro YUASA*, Moriyasu TAKARADA*,
Akitsugu NADAI** and Yukiharu HISAKI***

Abstract : Observations of sea surface currents by HF radar were carried out in Okasa Bay in autumn 1995. The overall characteristics of the major tidal currents (M_2, S_2, K_1, O_1) in Osaka Bay are examined. At the same time, variability of current and the clockwise residual circulation is investigated over spring-neap tidal cycle. It is found that magnitude and spatial scale of a clockwise residual circulation in the central part of Osaka Bay at spring tides are larger than that at neap tides. Furthermore, it is sugested that the southward flow at flood tide in the central part of Osaka Bay does not exist during neap tides.

Key words : *HF radar, tidal current, residual current*

1. Introduction

A high frequency ocean radar (HF radar) is a quite useful instrument which enables us to make a long term observation of sea surface current in the wide area. In last decade, a number of observations by HF radar have been made to analyze coastal phenomena such as tidal and residual currents (PRANDLE, 1987), frontal structure (MATTHEWS *et al.*, 1993), upwelling (SHKEDY *et al.*, 1995), and so on.

Okinawa Radio Observatory of Communications Research Laboratory (CRL) developed the first HF ocean radar system in Japan in 1988 (IGUCHI *et al.*, 1989) and the second one in 1991. OHNO (1991, 1993) made several current and sea state observations using HF radars at Tokara Strait, Japan Sea and other places. TAKEOKA *et al.* (1995) utilized the current measurement by HF radars to analyze the Kyucho in the Bungo Channel.

As shown in Fig.1, Osaka Bay is a semi-enclosed basin where the tidal current dominates and the residual flow plays an important role in the long term dispersion of material. Furthermore, it is known that a clockwise residual circulation exists in the central part of Osaka Bay (YANAGI and TAKAHASHI, 1988, 1995 : FUJIWARA *et al.*, 1989 : YUASA, 1994, e.t.c.). In order to obtain the detailed structure of these currents, a long-term observation of currents in wide area is necessary. However, most of the past current observations in Osaka Bay were point-wise measurement by current meter or temporary measurement of vertical section by Acoustic Doppler Current Profiler (ADCP) at best. Therefore, we adopted current measurements by the HF radars to the opbservation of tidal current and residual circulation in Osaka Bay. In the present work, we will illustrate the characteristics of the tidal currents, and variability of current and a clockwise residual circulation over spring-neap tidal cycles in Osaka Bay.

2. Specifications of the HF Radar and Observations

Current measurements by the HF ocean radar system were carried out at the two sites

* Chugoku National Industrial Research Institute, 2-2-2 Hiro-Suehiro, Kure, Hiroshima 737-0197, Japan
** Communications Research Laboratory, 4-2-1 Nukui-Kitamachi, Koganei, Tokyo 184-8795, Japan
*** Okinawa Radio Observatory, Communications Research Laboratory, 829-3 Aza-kuda, Nakagusuku-son, Nakagami-gun, Okinawa 901-24000, Japan

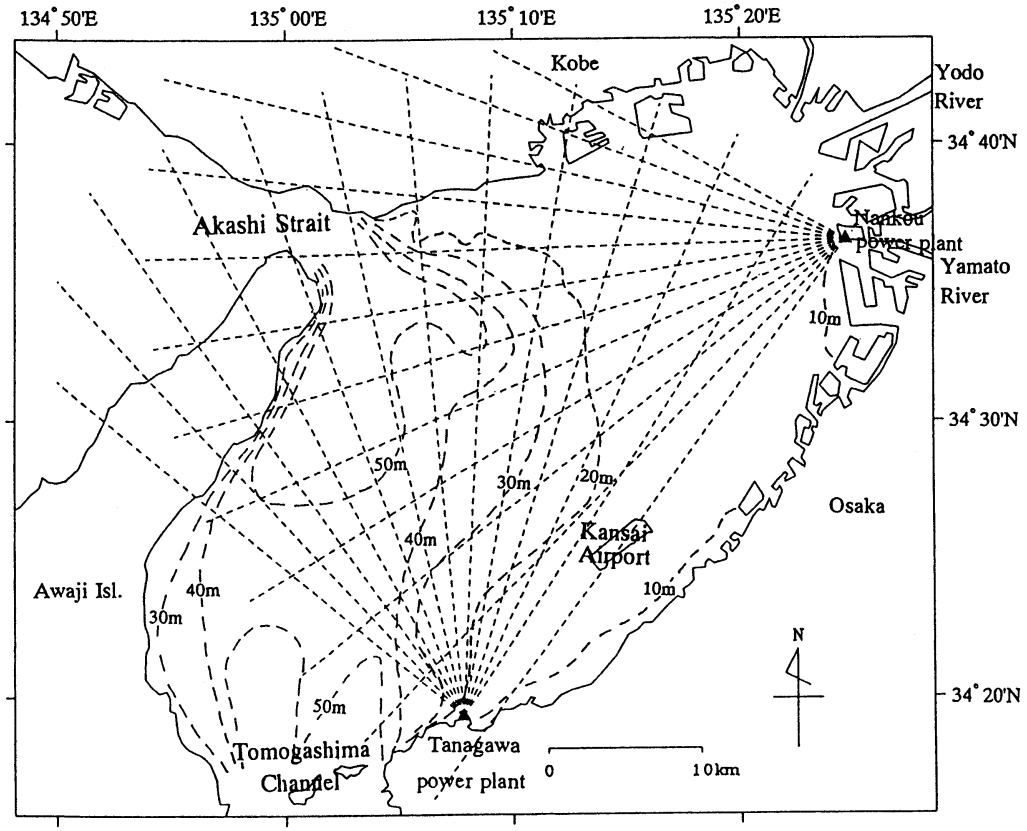

Fig. 1. Map of Osaka Bay. Broken curved lines are depth contours. Numerals are depth in meter. Straight broken lines shows the radar beams.

Table 1. Specifications of the HF ocean radar of CRL. After TAKEOKA *et al.* (1995)

Radar type	Frequency Modulated Interrupted Continuous Wave (FMICW) radar
Center frequency	24.515 MHz
Range resolution	1.5 km
Transmit power	100 W (peak), 50 W (average)
Antenna type	10-element phased array antenna
Beam width	15°
Beam directions	±45° (13 directions)

shown in Fig. 1, from 11 November to 12 December 1995. Two spring tides (23 Nov. and 7 Dec.) and two neap tides (15 and 29 Nov.) were included in this period. Table 1 shows the specification of the HF ocean radar system of CRL. A phased array antenna of 60 m long is used and the radar beam can be steered electrically in the direction within ±45°. Sea echoes over the range of 90 km can be detected under a favorable condition. Harder the wind blows, shorter the maximum observable range becomes, since sea waves impede the radio wave propagation. The radio wave is backscattered by sea surface waves with half the wave length of the radio wave. The measured current velocity represents the integrated value over the surface layer effective in advecting the surface waves. The thickness of this effective surface layer is said to be about $1/4\pi$ of the surface wave length and hence $1/8\pi$ of the radio wave

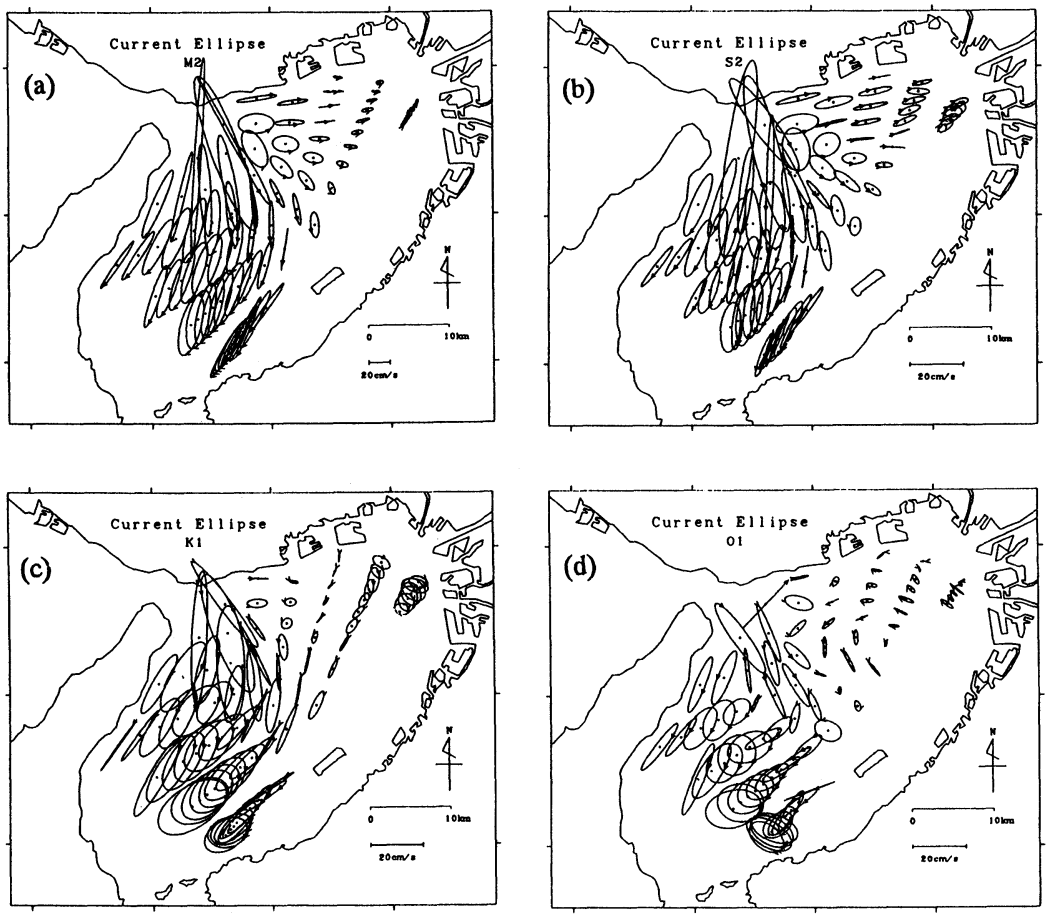

Fig. 2. Tidal current ellipses of major 4 components. (a) is M_2, (b) S_2, (c) K_1 and (d) O_1 tidal current.

length (STEWART and JOY, 1974), and it is about 0.5 m for the radars of CRL since the radio wave length is 12 m. Readers are referred to IGUCHI *et al.* (1989) and OHNO (1991) for more details of the radar hardware.

Backscattered signals along one beam were recorded for 2 minutes, followed by 3 minutes of the interval. This interleaving procedure has 5 minutes intervals, thus measurements along 12 separate beams can be made at hourly intervals.

3. Data Analysis and Observation Results

Obtained signals were spectrally analyzed and radial currents were determined. Here, since data obtained time was different by beam to beam at one site, radial currents were interpolated to the currents at every hour on the hour using linear interpolation method. From these values, hourly current vectors at cross points of radar beams were estimated.

3.1 Harmonic Constants

Harmonic analysis was carried out at each cross points and harmonic constants of 10 major tidal constituents (K_1, O_1, P_1, Q_1, M_2, S_2, K_2, N_2, M_4, MS_4) were obtained with use of the least square method (ODAMAKI : 1981). Tidal ellipses of M_2, S_2, K_1 and O_1 (major 4 components) are shown in Fig. 2(a), (b), (c) and (d), respectively. M_2 tidal current is most dominant component and phase progresses from near coast to central part. Amplitude of M_2 tidal current reaches about 70 cm/s near the Akashi

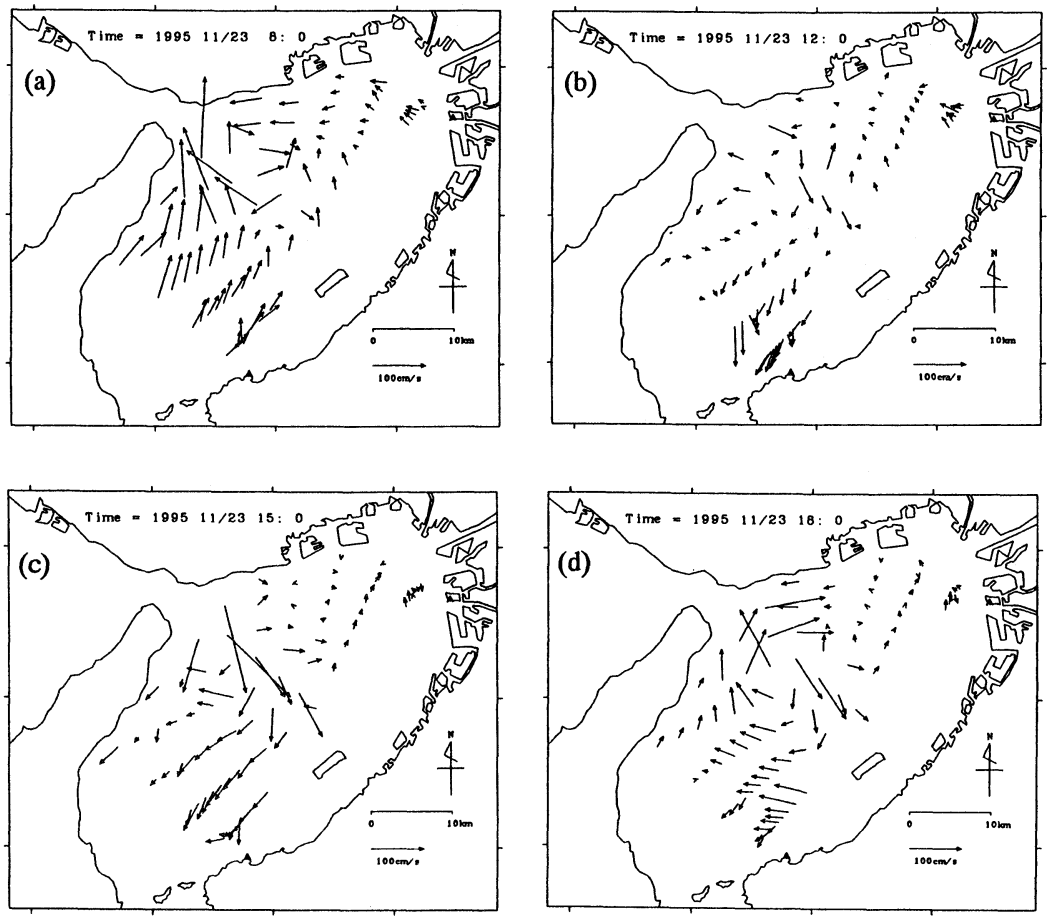

Fig. 3. Time series of the current vectors on 23 November 1995 (spring tide).
(a) flood tide, (b) slack after flood tide, (c) ebb tide, (d) slack after ebb tide.

Strait. Amplitude of S_2 tidal current is about half of that of M_2 tidal current, but flatness, direction of major axia and phase of S_2 tidal current ellipses in the area where depth is more than 20 m (the deeper area, see Fig. 1) are similar to M_2 tidal current. On the other hand, in the area where depth is less than 20 m (the shallower area), S_2 tidal current gradually becomes weak with the approach to the bay head whereas M_2 tidal current rapidly becomes weak. Amplitude of K_1 tidal current is weaker than that of S_2 near the Akashi Strait but stronger near the Tomogashima Channel. Flatness ratio of K_1 tidal ellipses in the shallower area becomes small with the approach to the bay head although that of other components does not change or becomes large. O_1 tidal current is the weakest component among the four major components. Its amplitude reaches about 16 cm/s near the Akashi Strait and about 15cm/s near the Tomogashima Channel. Amplitude of the semi-diurnal tidal currents (M_2 and S_2 components) become weak as approaching from the Akashi Strait to Tomogashima Channel. On the other hand, amplitude of the diurnal tidal currents (K_1 and O_1 components) is not so different between near the Akashi Strait and the Tomogashima Channel, although once that become weak off shore the Kansai Airport.

3.2 Time Series of the Current

In this paper, the time at which westward velocity at the Akashi Strait becomes maximum

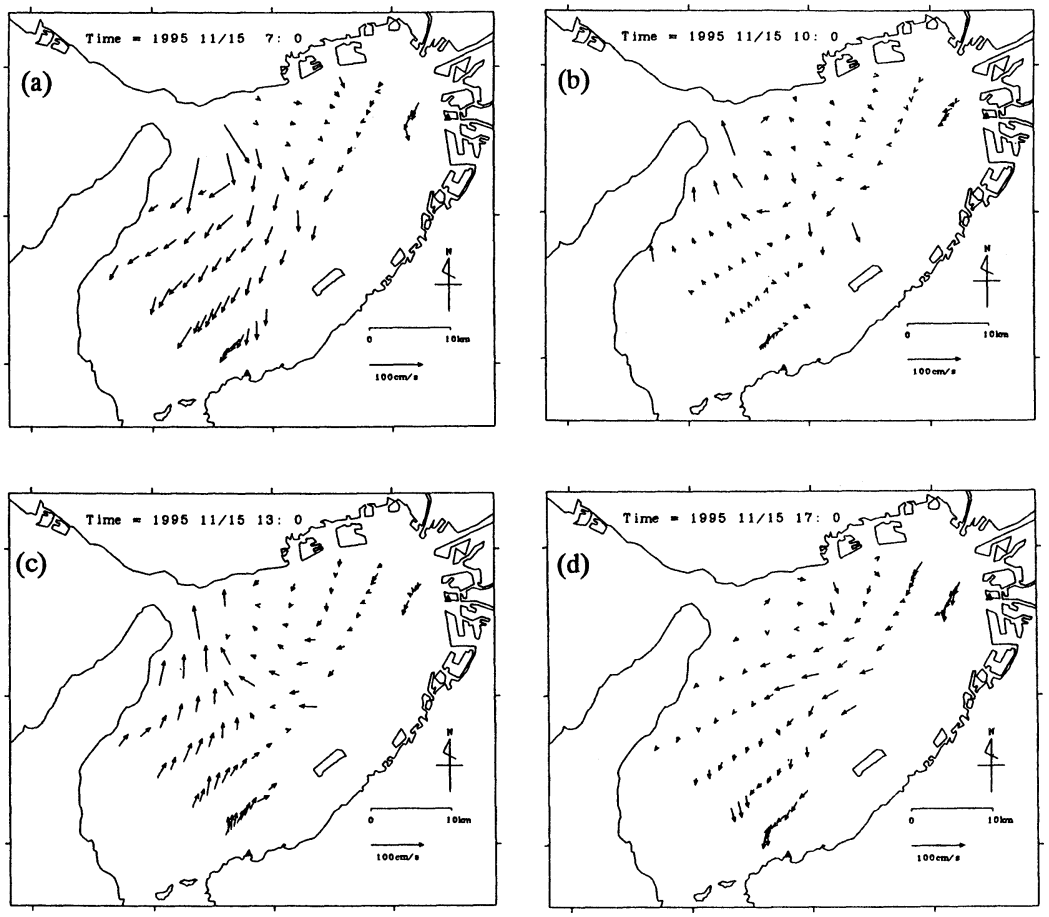

Fig. 4. Time series of the current vectors on 15 November 1995 (neap tide).
(a) ebb tide, (b) slack after ebb tide, (c) flood tide, (d) slack after flood tide.

speed is called flood tide and the time at which eastward velocity becomes maximum is called ebb tide.

Figure 3 shows the time series of the surface current vectors at flood tide (a), the slack after flood tide (b), ebb tide (c) and the slack after ebb tide (d) on 23 November 1995 (spring tide). From this time series, we can see how the semi-diurnal current develops in Osaka Bay. Maximum velocity reaches about 155 cm/s at flood tide and about 180 cm/s at ebb tide near the Akashi Strait. The surface current at the deeper area is stronger than that at the shallower area. A clockwise eddy is found in the central part of Osaka Bay at the slack (Fig. 3 (b) and (d)), although the intensity at the slack alfter flood tide is stronger than that at the slack after ebb tide. In spite of flood tide, southward flow has been said to exist at central part of Osaka Bay from the past knowledge (FUJIWARA *et al.*, 1989) and this flow is indeed found in Fig. 3 (a).

Figure 4 shows the time series of the current vectors at ebb tide (a), the slack tide after ebb tide (b), flood tide (c) and the slack tide after flood tide on 15 November 1995 (neap tide). The figure shows that the semi-diurnal current develops in Osaka Bay. Maximum velocity reaches about 110 cm/s at ebb tide and about 70 cm/s at flood tide near the Akashi Strait. Storong surface current is distributed in the deeper area. A clock-wise eddy is found in the central part of Osaka Bay at the slack after ebb tide (Fig. 4 (b)). These results correspond to

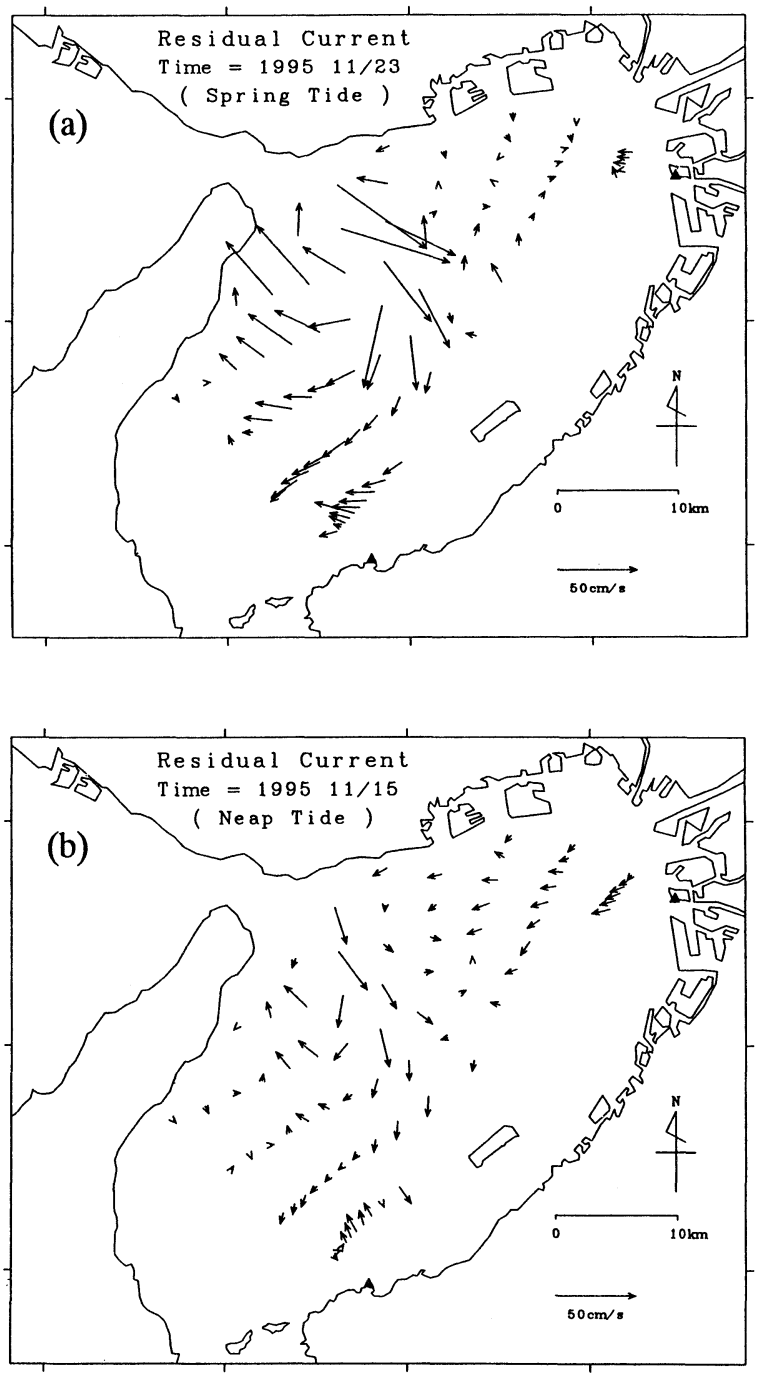

Fig. 5. Distribution of the residual current at spring tides (a) and neap tides (b).

that of spring tides with the intensity of currents put aside. However, southward flow at the flood tide is not found in Fig. 4 (c). Here, most of past observations were carried out during spring tides and the observation during neap tides was rarely made in Osaka Bay. This fact suggests that the southward flow existing at flood tide does not exist during neap tides. Furthermore, at the slack after flood tide of neap tides, we can not find a clockwise eddy in Fig. 4 (d). This clockwise eddy may be a fundamental flow structure of Osaka Bay. Namely, there is a possibility that the residual circulation fluctuates with lunar age period. Thus, we will investigate the variability of the residual circulation in the spring to neap tidal duration in the next section.

3.3 Residual Circulation during Spring Tides and Neap Tides

Figure 5 shows the circulation patterns which are obtained by averaging the current velocities at the beam cross points over 25 hours at spring tide (a) and neap tide (b). A clockwise residual circulation develops in the central part of Osaka Bay at both spring and neap tides. Maximum velocity of the circulation reaches about 70 cm/s during spring tides and about 30cm/s during neap tides near the Akashi Strait and the overall residual velocity during spring tides is 2–3 times stronger than that during neap tides.

The positions of western, northern and eastern edges of a clockwise circulation are not so much different between spring and neap tides. However, during spring tides, a clockwise circulation spreads more to south than that during neap tides. Most likely, this is because the western edge of a clockwise residual circulation is constrained by the northern part of the Awaji Island whereas northern and eastern edges are constrained by the slope which becomes deep rapidly from 20m to 50m depth (refer to Fig. 1), leaving only southern edge free from such topographic constriction. That is, spatial scale of this circulation at spring tides is larger than that at neap tides.

4. Discussions and Conclusions

Variability of current and a clockwise residual circulation are investigated over spring to neap tidal cycles in Osaka Bay using the observation results by HF radar. As a result, it is suggested that the southward flow at flood tide in the central part of Osaka Bay exists during spring tides but not during neap tides. However, this southward flow can be seen during neap tides of 29 November 1995 (not shown). Here, the tidal range at the tide station of Osaka (34°39′N, 135°26′E) is about 61 cm at morning of 15 November and 83 cm at morning of 29 November with a difference of about 22 cm for the same neap tide condition. This fact suggests that, although under the neap tides, there are two cases where the southward flow at flood tide does or does not develop in the central part of Osaka Bay depending on the tidal range at the neap tidal period. This phenomenon will be studies more in the near future using a numerical model.

FUJIWARA *et al.* (1989) investigated the variability of a clockwise residual circulation in the central part of Osaka Bay with use of ADCP observed data. They suggested that intensity of the residual circulation fluctuated according to the fluctuation of the maximum velocity of tidal current at the Akashi Strait. In our results, intensity of a clockwise circulation at apring tides is stronger than that at neap tides. That is, their suggestion corresponds to our result. Furthermore, in our results, intensity of a clockwise eddy at the slack after ebb tide (Fig. 3 (d)) is stronger than that at the slack after flood tide (Fig. 3 (b)) during spring tides. On the other hand, during neap tides, we can find a clockwise eddy at the slack after ebb tide (Fig. 4 (b)), but we cannot find that at the slack after flood tide (Fig. 4(d)). This fact suggests that a clockwise eddy at the slack is caused effectively by the eastward flow at the Akashi Strait and should contribute to compose a clockwise residual circulation in the central part of Osaka Bay.

Acknowledgments

The authors express their sincere thanks to The Kansai Electric Power Co., Inc. for borrowing site to set the radar systems and to Prof. N. HAYAKAWA of Nagaoka Univ. Tech. and Dr. K. ASAI of Yamaguchi Univ. for their helpful

suggestions.

Reference

FUJIWARA, T., T. HIGO and Y. TAKASUGI (1989) : Const ant flow, tidal current and water circulation in Osaka Bay. Proc. Coastal Engin., JSCE, **36**, 209–213 (in Japanese).

IGUCHI, T., T. UMEHARA, Y. OHNO and K. KOZAKI (1989) : Observation of ocean currents and sea state with an HF ocean radar. Rev. com. Res. Lab., **35**, 387–397 (in Japanese).

MATTHEWS, J. P., A. D. FOX and D. PRANDLE (1993) : Radar observation of an along-front jet and transverse flow convergence associated with a North Sea front. Cont. Shelf Res., **13**, 109–130.

ODAMAKI, M. (1981) : A new trial on the harmonic analysis for short period observation of tide and tidal current, using the least square method. Report of Hydrogr. Res., **16**, 71–82 (in Japanese).

OHNO, Y. (1991) : HF ocean radar observations of ocean current. J. Com. Res. Lab., **38**, 377–385.

OHNO, Y. (1993) : Present stage of the HF ocean radar at Communications Research Laboratory and results of experiments. Navigation, **116**, 62–68 (in Japanese).

PRANDLE, D. (1987) : The fine-structure of nearshore tidal and residual circulations revealed by H. F. radar surface current measurements. J. Phys. Oceanogr., 17, 231–245.

SHKEDY, Y., D. FERNANDEZ, C. TEAGUE, J. VESECKY and J. ROUGHGARDEN (1995) : Detecting upwelling along the central coast of California during an El Nino year using HF-radar. Cont Shelf Res., **21**, 803–814.

STEWART, R. H., and J. W. JOY (1974) : HF radio measurements of surface currents. Deep-Sea Res., **21**, 1039–1049.

TAKEOKA, H., Y. TANAKA, Y. OHNO, Y. HISAKI, A. NADAI and H. KUROIWA (1995) : Observation of the Kyucho in the Bungo Channel by HF radar. J. Oceanogr. **51**, 699–711.

YANAGI, T. and S. TAKAHASHI (1988) : Residual flow in Osaka Bay. Bull. on Coastal Oceanogr., **26**, 66–70 (in Japanese).

YANAGI, T. and S. TAKAHASHI (1995) : Variability of the residual flow in Osaka Bay, Japan. Mem. Fac. Engin, Ehime Univ., **14**, 377–391.

YUASA, I. (1994) : Residual circulation, coastal fronts and behavior of nutrients in the Inland Sea. Rep. Chugoku Nat. Ind. Res. Inst., **12**, p184 (in Japanese).

Received August 17, 1999
Accepted December 24, 1999